Creep Behavior of Orthogonal Rib Box Floor of Poplar Laminated Veneer Lumber

Yan Liu,* Jijia Long, Jing Chen, Xingyu Song,* and Wenbo Jia

Poplar laminated veneer lumber (LVL) orthogonal rib box floor is a new type of floor composed of orthogonal LVL rib beams and oriented strand board (OSB). To study the creep performance of the box floor, four 3600 mm × 4800 mm floor specimens were designed and manufactured. The creep tests of the box floor with local damage, repeated load, and different stress ratio loads were conducted. The creep of the floor increased with ambient temperature and humidity. Because of the local damage of the box floor, the creep increased. Repeated loading increased the creep deformation of the floor, and increasing the load accelerated the creep of the floor. Combined with the creep mechanism of wood materials, a creep theoretical calculation formula of the box floor with LVL orthogonal ribs was established. Comparing the creep model analysis with the test data, it was found that the modified Burger mode can well simulate the creep performance of LVL box floor. Therefore, the modified Burger model can be used to calculate the creep deformation of the box floor.

DOI: 10.15376/biores.17.4.6158-6177

Keywords: Orthogonal ribbed beam box floor; Creep test; Creep model; Finite element simulation; Creep prediction

*Contact information: College of Civil Science and Engineering, Yangzhou University, Yangzhou, Jiangsu 225127, China; China; *Corresponding authors: ppsxy@163.com;liuyan@yzu.edu.cn*

INTRODUCTION

Poplar laminated veneer lumber (LVL) is a kind of engineering wood that is made from raw poplar by rotary cutting, drying, coating, veneer striation, and hot pressing. In addition to its excellent performance, it has better mechanical properties than natural poplar wood (Liu *et al*. 2017). There have been many studies on the mechanical properties of LVL members and structures, but few studies on their creep properties. A great deal of investigation has been carried out to understand the relationship between creep deformation and molecular structure. Mature creep theory seeks to simplify the wood polymer to reveal its rheological characteristics. Armstrong *et al*. (1960, 1961) proposed that changing moisture content affects wood creep properties. Schniewind (1967) found that periodic variations in relative humidity and temperature in the environment decreased the average time it took for small Douglas fir beams to fail. Aipo (2000) studied the bending creep of LVL, plywood, spruce I-beam, and other components after different anti-corrosion treatments for up to eight years under natural environment and low stress levels. When the stress level is low, the creep increases with the increase of stress, and the creep and time are in the form of power function. Yazdani *et al.* (2003) studied T-section LVL simply supported beams by full-scale model test under natural environment. The loading time was 895 days, and then the creep recovery stage was observed for 90 days. The Burger model can well fit the creep test results and verify the accuracy of the model. The parameters of

the Burger model are obtained according to the creep test results. Dinwoodie *et al.* (1992) studied the creep properties of wood composites, finding that the relative creep increased slightly and linearly with respect to stress within the range of stress levels adopted, as well as increasing with severity of the environment. All materials showed greater sensitivity to alternating humidity than to alternating temperature. Pierce *et al.* (1979) studied the creep properties of wood composites, finding that the Burger model with an additional viscous damper element had higher prediction accuracy. Leichti and Tang (1989) carried out the creep test of I-shaped timber beams and conducted a comparative analysis of the creep of reinforced and unreinforced timber beams. Under long-term load, the stiffness of the reinforced timber beam changes little and has good creep performance.

Zhu and Zhou (2009) studied the influence of LVL creep on structural stability, and obtained the tensile-compression creep law of LVL material under normal use environment in China. They established the LVL creep constitutive model and the creep buckling finite element model of wood structure under long-term deformation. Chen (2017) found that the loading level, cross-section form, and reinforcement ratio prestress value can affect the long-term bending performance of wood beams. With the help of power law model, the value of creep deformation coefficient was obtained. Cao (2017) conducted three groups of creep tests of plywood beams with different stresses and selected the modified Burgers model as the constitutive model of plywood. The creep characteristic constant of larch plywood beam was obtained by fitting the test data with the modified Burgers model. This model has good fitting accuracy and it can be used to predict the short-term creep of plywood beams. Zuo *et al.* (2021) compared the long-term flexural performance of laminated timber beams strengthened with different replacement proportions and loads by experiments. It was found that when the replacement rate is constant, with the increase of loading value, the initial deflection and creep value of laminated timber beams increases, and with the increase of load, the deformation rate increases. When the loading ratio is fixed, the deflection deformation can be reduced by increasing the replacement proportion of the reconstituted bamboo in the plywood beam. Yang *et al.* (2017) studied the long-term bending performance of prestressed plywood beams under the same prestress, different number of prestressing tendons, the same number of prestressing tendons, and different prestress. It was found that prestress regulation can effectively reduce the creep of wood beams. Zhou *et al*. (2020) conducted creep tests on steel-wood composite floors under long-term load. The combination of the two materials can give full play to the advantages of materials, so that the floor has good integrity and bearing capacity.

Wang *et al.* (2020) designed and made three wood beams strengthened with CFRP bars to study their mechanical properties under long-term load. The initial defects of wood beams affect the long-term performance, and the deflection of wood beams without initial defects is smaller than that of wood beams without reinforcement. The deflection of reinforced beam with obvious initial defects in midspan was higher than that of unreinforced beam, and obvious cracks appeared around the midspan joint. He *et al.* (2016) studied the number of prestressed tendons, prestress, load, and other factors on the long-term bending performance of prestressed plywood bamboo beam. Increasing the number of prestressed tendons can reduce the creep, and when the number of prestressed tendons increases to a certain number, the effect on reducing creep is no longer obvious. Increasing prestress can reduce the creep of bamboo beam; the greater the load, the greater the creep. According to the test results, the long-term stiffness calculation formula of bamboo beam is deduced. Sheng (2015) conducted creep tests on three poplar LVL columns with the same size, and applied stress ratios of 0.1, 0.3, and 0.5 to study the effects of different load sizes

on the strain and deflection of poplar LVL columns. The specimen basically conforms to the creep law of wood. The larger the stress ratio, the greater the creep and the greater the deflection in the column. According to the wood creep mechanism, the creep model of poplar LVL column was established and the creep equation was obtained. Liu (2018) applied 0.3 and 0.5 failure loads to four LVL beams of poplar with 75 mm width, 125 mm height, and 2400 mm length for 110 days of creep test. Under the same load, the creep of wood beams parallel to the adhesive layer direction was smaller, where the greater the stress ratio, the greater the creep.

Previous research on the creep characteristics of timber and engineering wood structures provide a valuable reference for this paper. Through the creep test of poplar LVL orthogonal ribbed box floor and the series research on the mechanical performance of the box floor, the results may provide technical support for the application of poplar LVL orthogonal ribbed box floor in building structures.

EXPERIMENTAL

The size of the floor specimen was 3600 mm × 4800 mm. The parameters of the floor specimens are shown in Table 1 and in Figs. 1 and 2. The internal rib beam joints of each sample adopted the 3 mm thick Q235 steel L-shaped connector, which was connected by M4 × 20 mm cross-countersunk self-tapping screws. The size of connectors and the number of screws were increased at the end nodes of the rib beam, which were connected to the edge-sealing rib beam by M4 × 40 mm cross-countersunk self-tapping screws. OSB plates were used as the upper and lower floor slabs of the box floor, which were connected to the rib beam by 2.8 × 50 mm round nails. The spacing between the round nails was 150 mm and 300 mm at the edge-sealing rib beam and the internal rib beam, respectively (Su *et al*. 2022).

The creep characteristics of the box floor under local damage loading, repeated loading, and different stress ratios were studied. During the short-term loading test of specimen L2-1, when the load reached 15 kN/m^2, the OSB joint in the middle area of the floor bottom was separated by 3 to 4 mm, but the whole specimen was not seriously damaged, and still maintains good integrity. Poplar LVL box floor was placed on the steel base. A water tank for loading as placed on the upper part of the floor. To ensure the safety of the water tank, a reinforced steel frame was set around the water tank, and the loading device is shown in Fig. 2. To keep the load constant in the creep test, a waterproof film was coated on the water surface inside and on the top of the water tank to prevent water evaporation, and the water surface height was regularly checked during the creep test to ensure that the load value remains unchanged. The creep test load and the relationship between load and duration are shown in Table 2 and Fig. 3, respectively.

Table 1. Floor Specimen Number and Parameters

Specimen	Specimen Size (mm)	Long Side Rib Beam Spacing (mm)	Short Rib Beam Spacing (mm)	Section Size of Rib Beam (mm)	Comparison
L1-1	3600×4800	600	600	40×235	Control
L2-1	3600×4800	600	600	40×235	Local Damage
L2-2	3600×4800	600	600	40×235	Repeated Load
L2-3	3600×4800	600	600	40×235	Maximum Load
* L2-1 is specimen with local damage after short-term bending test.					

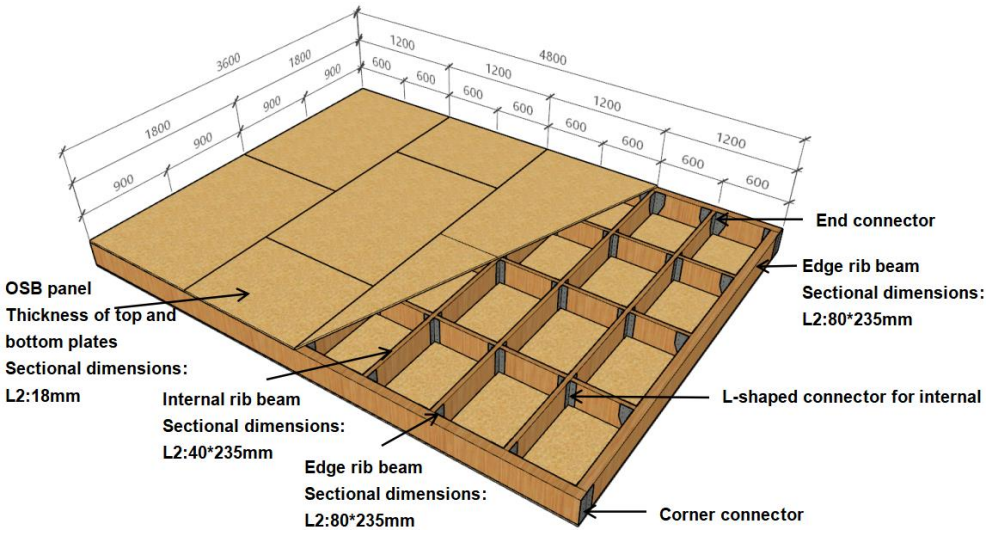

Fig. 1. Plane and detailed configuration of test specimen

(a) loading water tank and support base **(b)** Test overview

Fig. 2. Test setup

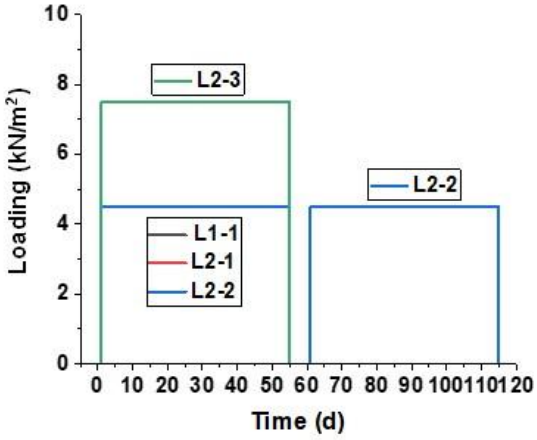

Fig. 3. Load-time relationship

Table 2. Floor Specimen Number and Parameters

Specimen	Load (kN/m^2)	Stress Ratio*	Time (d)
L1-1	4.5	0.3	55
L2-1	4.5	0.3	55
L2-2	4.5	0.3	55
L2-3	7.5	0.5	55
* The stress ratio is the ratio of the creep load applied by the specimen to the maximum load of the short-term loading test of the specimen.			

Experimental Scheme and Measuring Arrangement

A TS3860 type static resistance strain gauge was used to record the floor deflection change during creep test, and a CX601 type industrial high-precision thermometer and hygrometer were used to record the environmental temperature and humidity change, as shown in Fig. 4. To measure the creep deformation of each box floor specimen under long-term load, the displacement meter was arranged along the longitudinal and transverse axis of the floor. Based on the symmetry of the box-type floor and the symmetry of the load, a quarter of the floor area was selected for the layout range of the displacement meter. The distribution of each measuring point is shown in Fig. 5(a), and the number of the displacement meter is W1 to W14. The layout of the displacement measuring point of the specimen is shown in Fig. 5(b).

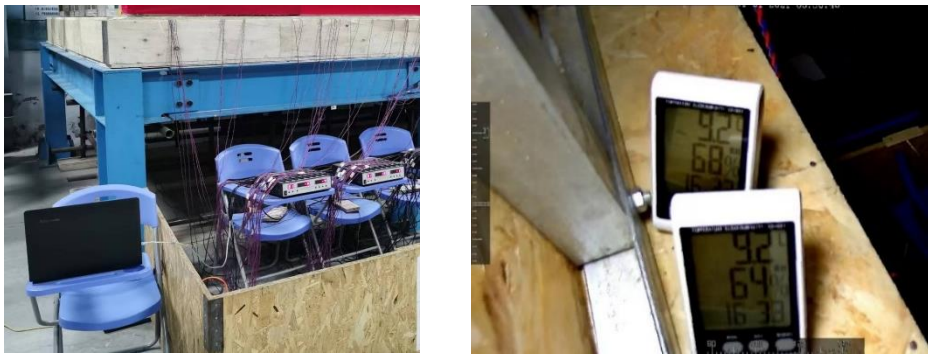

(a) Static resistance strain gauge **(b)** Temperature and humidity meter

Fig. 4. Measuring equipment

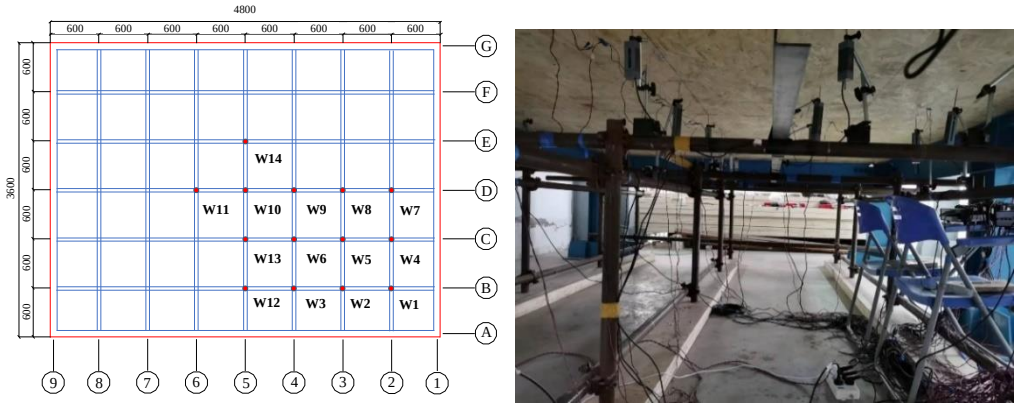

(a) Plan of displacement measuring points **(b)** Installation of displacement meter

Fig. 5. Design and arrangement of displacement measuring points

RESULTS AND DISCUSSION

Temperature and Humidity Record

The creep test time of each specimen was 55 days, and the ambient temperature and humidity were recorded regularly during the test. In the first week of the experiment, the data were recorded every 2 hours, and then every 4 hours. The temperature fluctuation range in the environment during the test was 6.2 to 14.4 °C, and the humidity fluctuation range was mainly in the range 33 to 98%, as shown in Fig. 6.

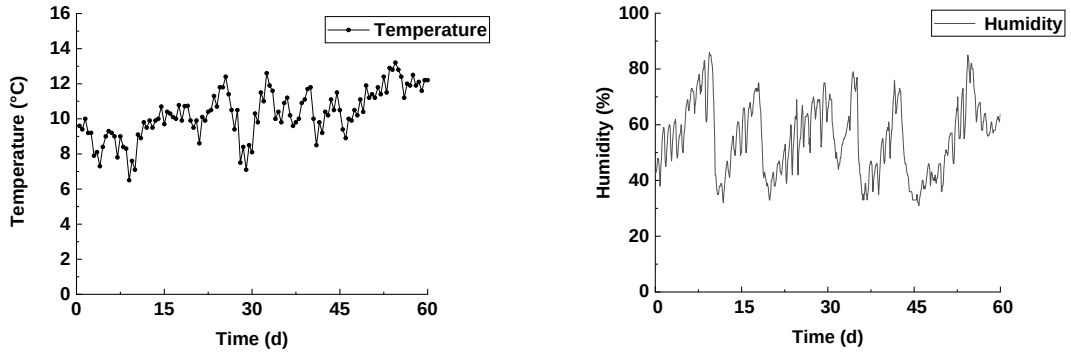

(a) Specimen L1 - 1

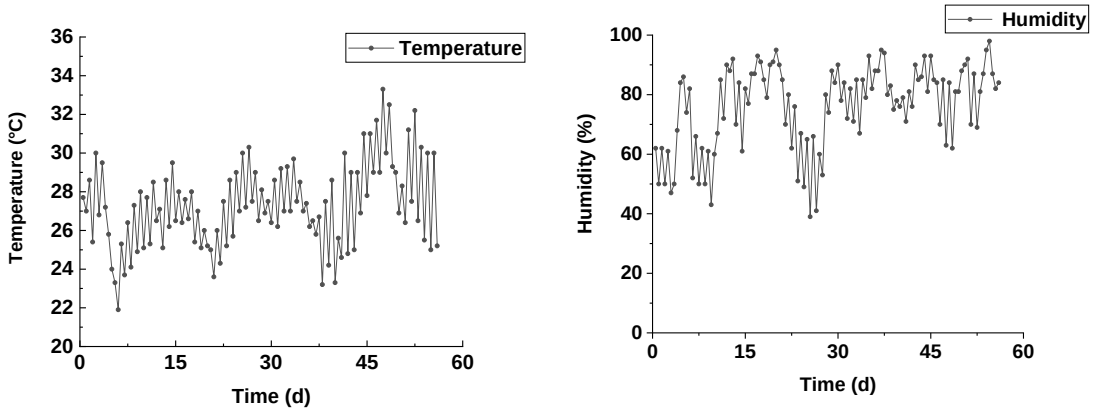

(b) Specimen L2 - 1

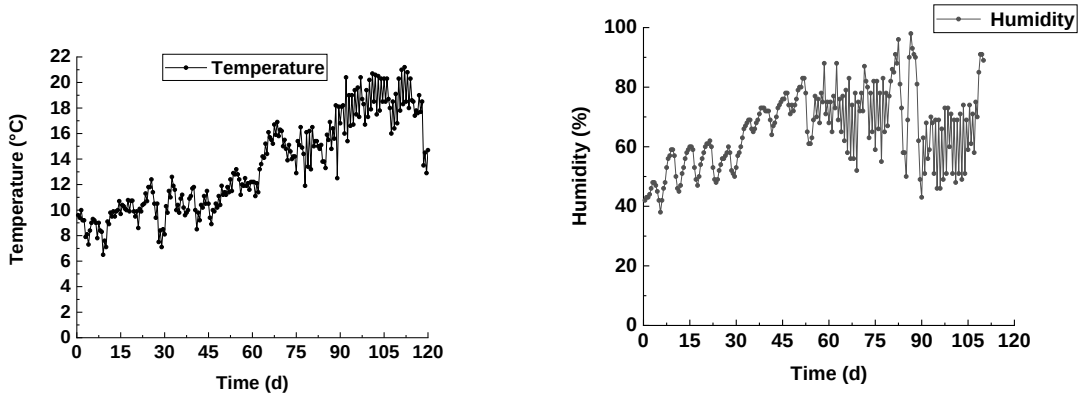

(c) Specimen L2 - 2

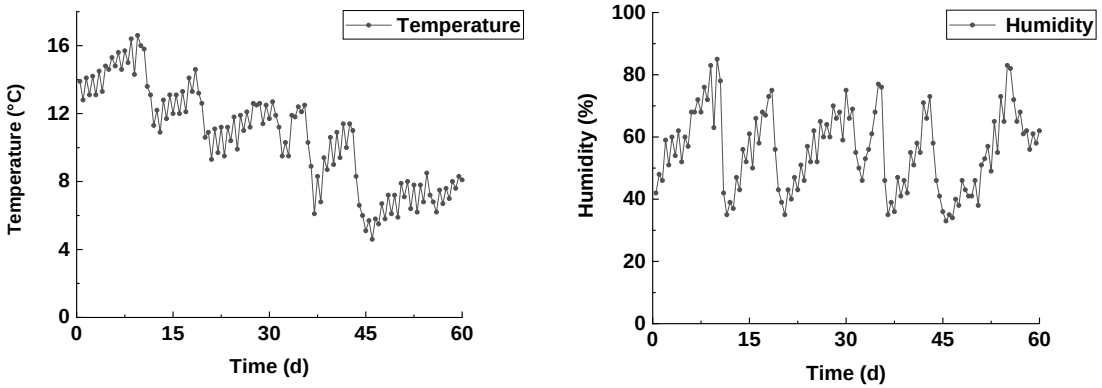

(d) Specimen L2 - 3

Fig. 6. Change of temperature and humidity during the test

Floor Deflection

To determine the creep deformation of poplar LVL orthogonal rib box floor under load, the deflection-time relationship of each test point of specimens was drawn with time as the horizontal axis and the deflection of the test point as the vertical axis, as shown in Fig. 7.

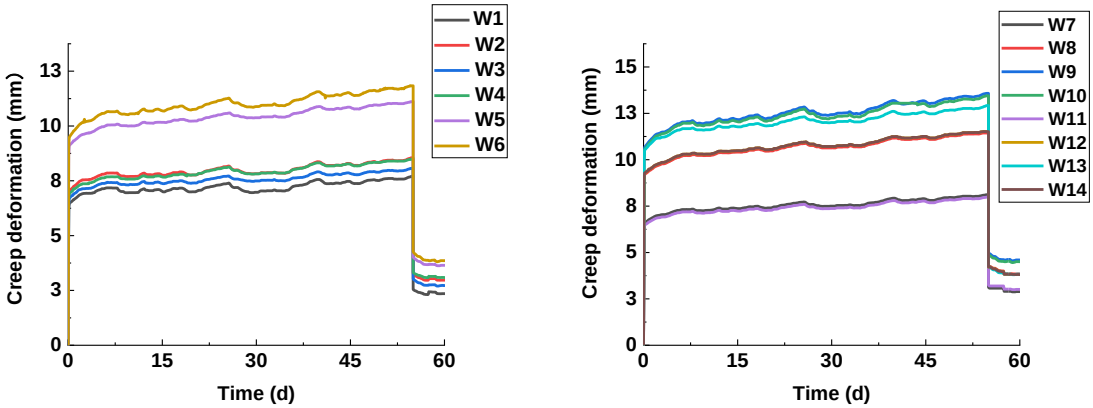

(a) Specimen L1 - 1

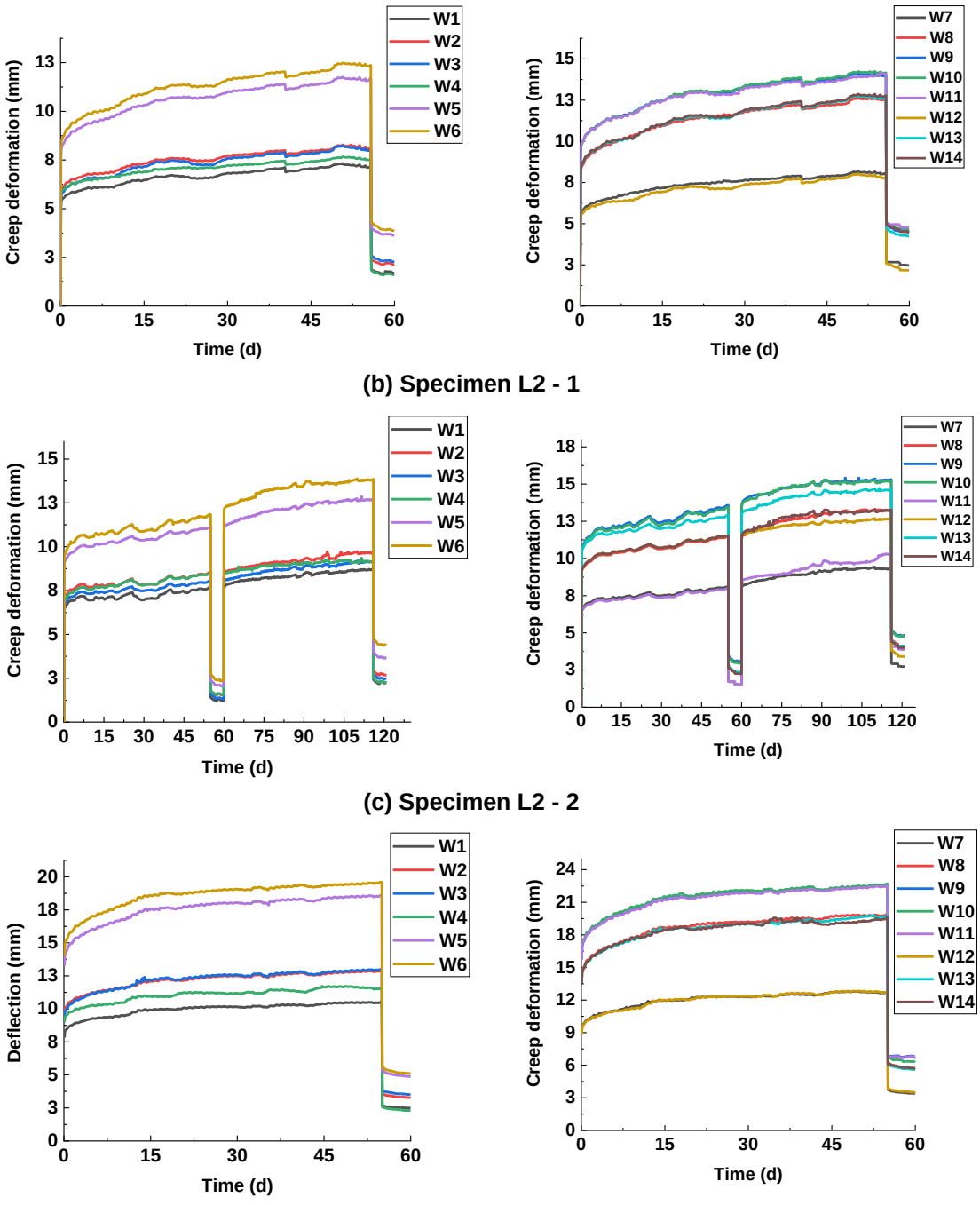

Fig. 7. Creep deflection–time curve

Figure 7 reveals that the creep process of the test specimen could be divided into two stages: the instantaneous deformation stage, which produces elastic deformation when the load is just applied to the specimen; and the second stage that is the creep stability stage, in which the specimen has viscoelastic and viscous deformation. When the applied long-term load is small (Table 2), the deformation increases limited with time. The creep deformation of each measuring point of the floor gradually increases with time from about the first 15 days after the load is applied. When the specimen entered the creep stability period, the creep growth rate gradually decreased. Although the creep values at different

measuring points were different, the curves are basically parallel, indicating that the specimen has good integrity and stiffness. The deflection development law of each measuring point of the floor was the same, and the maximum deflection appeared in the middle of the whole floor specimen.

Figure 7 shows that when the test specimen was unloaded, the specimen had an immediate recovery of the deformation; with the extension of time, the specimen had a small amount of delayed recovery of deformation, that is, elastic aftereffect; finally, there was a certain amount of residual deformation, as shown in Table 3. Generally, the creep of wood materials consists of elastic deformation, viscoelastic deformation, and viscous deformation. The immediate recovery deformation of specimen is elastic deformation, and the elastic aftereffect that gradually recovers after unloading belongs to viscoelastic deformation, while the residual deformation is viscous deformation, which cannot be recovered after unloading (Jozsef and Benjamin 1982).

Table 3 shows that the residual deformation of W10 of specimen L2-3 increased by 38.9% compared with that of control specimen L1-1, indicating that the load had the greatest impact on the residual deformation of specimens. The W10 of the specimen with damage and repeated loading was also increased by 3% and 19.3%, respectively, compared with L1-1. The residual deformation of L2-2 with repeated loading includes the residual deformation after the first unloading, so the residual deformation after the second unloading is also large. When the load was small, the creep deformation of specimen L2-1 with damage increased to a limited extent compared with L1-1. The variation law of residual deformation of measuring points W7 and W12 was the same as that of W10, and the closer to the end of the specimen, the smaller the residual deformation of the specimen.

Table 3. Residual Deformation of 3 Measuring Points of Each Specimen

Specimen	Residual Deformation (mm)		
	W10	W7	W12
L1-1	3.85	2.56	3.38
L2-1	3.97	2.64	3.68
L2-2	4.77	2.74	3.80
L2-3	6.30	3.41	4.50

The change of creep deformation with temperature and humidity of W10 in specimen L1-1 to analyze the influence of ambient temperature and humidity on the creep performance of the specimen, is shown in Fig. 8. Figure 8(a) shows the relationship between creep deformation and humidity of specimen L1-1 when the temperature changes little. Figure 8(b) shows the relationship between creep deformation and temperature of specimen L1-1 when the humidity is basically equal. Figure 8 (c) shows the relationship between creep deformation and temperature and humidity of specimen L1-1 when the temperature and humidity both increase.

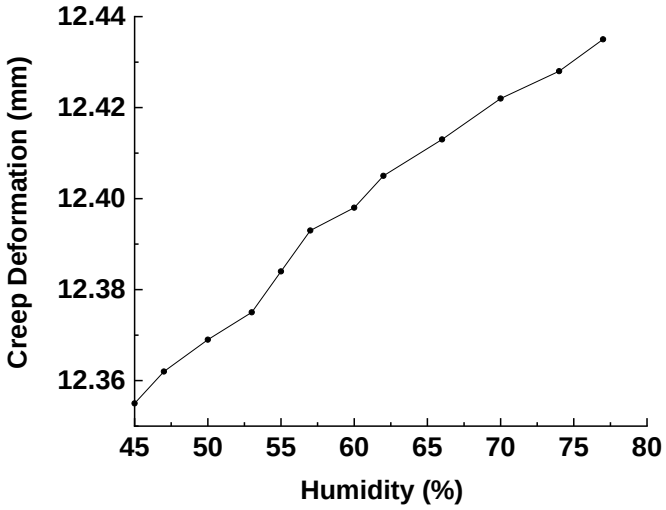

(a) Relationship between humidity and creep deformation

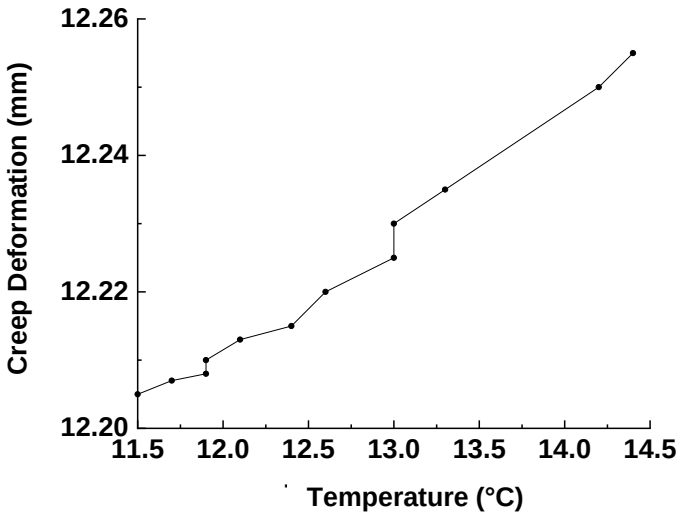

(b) Relationship between temperature and creep deformation

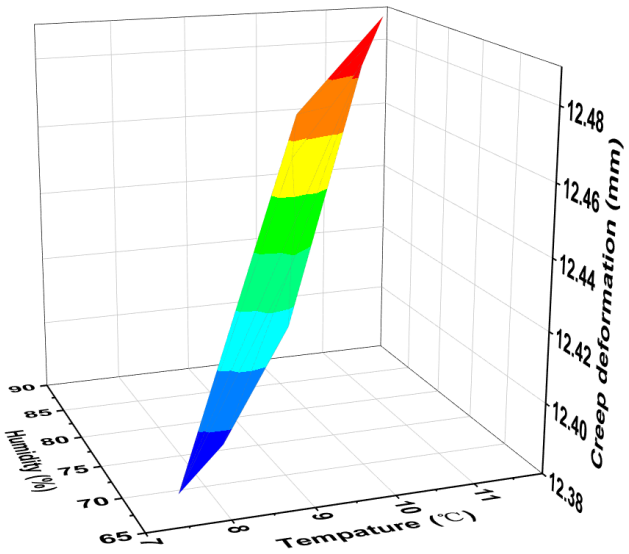

(c) Relationship between temperature and humidity with creep deformation

Fig. 8. The relationship between specimen creep deformation and temperature and humidity

The change of temperature and humidity will affect the creep deformation of the specimen. When the temperature was maintained at 12.6 ± 0.4 °C and the humidity increased by 22%, the deflection of measuring point W10 of specimen L1-1 increased by 0.08 mm, as shown in Fig. 8(a). When the humidity was maintained at 58 ± 2% and the temperature increased by 2.9 °C, the deflection of measuring point W10 increased by 0.05 mm as shown in Fig. 8(b). The creep deformation of box floor increased with the increase of environmental humidity, which indicates that environmental humidity affects the moisture content of wood and plays a role in increasing plasticity in the floor. With the increase of ambient temperature, the mechanical strength and stiffness of box floor may decrease, while the creep deformation of wood materials, especially viscoelastic deformation and viscous deformation, will increase to some extent (Jozsef *et al.* 1982).

Theoretical Analysis and Discussion

The creep deformation of measuring point W10 of specimen

The creep deformation-time relationship of the displacement measurement point W10 in the middle of the floor is shown in Fig. 9. Due to the presence of local damage, the initial deformation of specimen L2-1 was 0.140 mm larger than that of specimen L1-1, and with time, the creep deformation of specimen L2-1 was greater than that of control specimen L1-1. The local damage of specimen L2-1 reduced the stiffness of the floor and increased the creep.

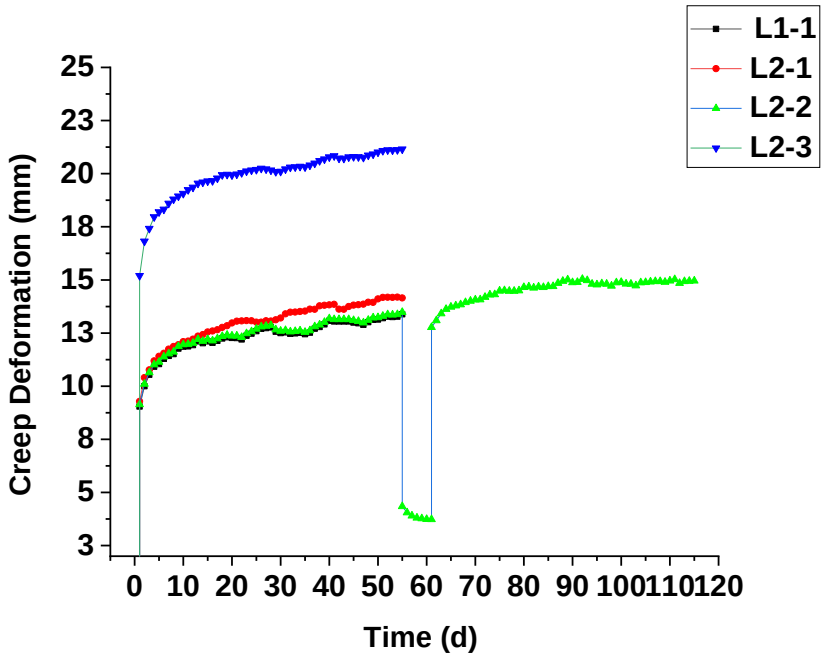

Fig. 9. Deflection-time curve of measuring point W10 of each specimen

Under the same load of 4.5 kN/m^2, the creep deformation of specimen L2-2 and L1-1 within 55 days was compared to explore the effect of repeated load on creep performance. It can be seen from Fig. 8 that the creep deformation of specimen L2-2 at the first loading was almost the same as that of specimen L1-1. In the first creep test, the residual creep deformation of specimen L2-2 after unloading was 3.73 mm. Due to continuous measurement, the residual deformation will accumulate into the creep deformation of the second load. This resulted in the creep deformation of specimen L2-2 at the second load being 14.95 mm, which is slightly larger than that of specimen L1-1 (13.38 mm) at the first load. However, under repeated loading, the creep rate of specimen L2-2 was 1.42 mm/d lower than that of specimen L1-1 (2.89 mm/d).

In Fig. 9, also comparing the creep time relationship between specimen L2-3 (load of 7.5 kN/m^2) and specimen L1-1 (4.5 kN/m^2), it can be seen that the greater the load applied by the specimen, the greater the creep deformation, and the increase of load will obviously affect the creep deformation of the specimen.

Relative Creep Deformation

To eliminate the influence of elastic deformation on creep analysis and compare the creep viscous deformation and viscoelastic deformation of each specimen, the relative creep deformation was defined as follows,

$$\omega = \delta_1 - \delta_0 \quad (1)$$

where δ_0 is initial elastic deformation, and δ_1 is creep deformation in t_1 time.

Under the same load of 4.5 kN / m^2, the relative creep deformation of each specimen within 55 days was compared, and the relative creep deformation-time relationship of the displacement measuring point W10 in the middle of the floor is shown in Fig. 10.

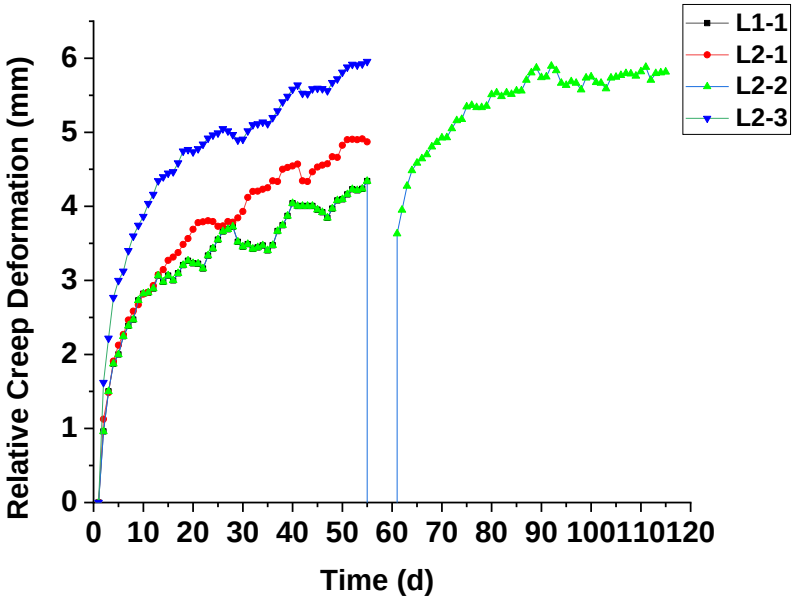

Fig. 10. Relative creep deformation of measuring point W10 in the middle of each specimen

As shown in Fig. 10, specimen L2-1 exhibited 4.865 mm relative deflection within 55 days, while specimen L1-1 exhibited 4.315 mm relative deflection. The relative deflection generated by creep test is due to the viscous elastic deformation and viscous deformation of the floor under constant stress. In specimen L2-1 with local damage, the relative deflection was 0.73 mm higher than in specimen L1-1. Because of the initial damage, the strength of the nail joint of specimen L2-1 decreased, reducing the stiffness of the floor. In comparison with the relative deflection of the W10 measurement point of the floor in the two creep tests, specimen L2-1 exhibited a greater viscous deformation and viscoelastic deformation.

Figure 10 shows that the relative creep deformation of specimen L2-2 was almost the same as that of specimen L1-1 within 55 days of the first loading. After the specimen L2-2 was loaded again, the relative creep deformation of the measurement point W10 was 5.81 mm, which was 33.87% higher (4.34 mm) than specimen L1-1. Due to the influence of residual deformation after the first unloading, the relative creep deformation of specimen L2-2 after the second loading increased.

In Fig. 10, comparing the relative creep deformation of specimen L2-3 and specimen L1-1, it can be found that the relative deformation of specimen L2-3 was 5.95 mm, which was 37.09% higher than that of sample L1-1. The magnitude of creep load was the most important factor that affects the relative creep deformation of the specimen.

Creep Coefficient

In structural design, the elastic deformation of the component is multiplied by the creep coefficient to estimate the creep deformation of the component in a certain time under long-term load. To analyze the creep performance of the specimen under long-term load, the creep coefficient $\varphi(t,t_0)$ was calculated as the ratio of the creep deformation of the specimen at a certain time to the initial elastic deformation, as follows.

$$\varphi(t,t_0)=\frac{\omega_{cr}(t,t_0)}{\omega_{cr}(t_0)} \quad (2)$$

where $\omega_{cr}(t,t_0)$ is creep deflection at *t* time, and $\omega_{ci}(t_0)$ is initial elastic deflection.

The creep coefficient-time relationship within 55 days of each specimen at W10 is shown in Fig. 11.

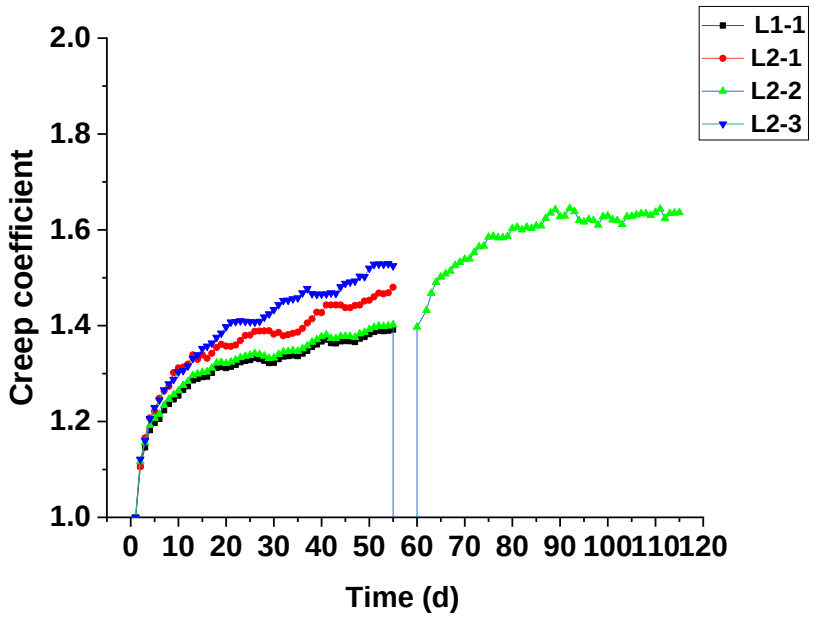

Fig. 11. Creep coefficient at W10 of each specimen

Figure 11 shows that under the same creep load, the creep coefficient of specimen L2-1 with local damage in the creep stability period was 1.48, which was noticeably higher than that of specimen L1-1 1.39. The creep test of specimen L2-1 was carried out after the local damage occurred in the short-term bending test joints of the specimen. The local damage that occurred in the specimen reduced its stiffness, and it led to the increase of creep deformation, and thus its creep coefficient increased.

Under the same load, the creep coefficient of specimen L2-2 after the first loading was basically the same as that of specimen L1-1, but the creep coefficient 1.64 after the second loading was much higher than that of specimen L1-1. This may be that the creep deformation of specimen L2-2 after the second loading included the residual deformation after the first unloading, making the creep coefficient larger.

The load of specimen L2-3 was the largest, and its creep coefficient 1.52 was also patently higher than that of sample L1-1. It shows that the load had the most effect on the creep performance of the specimen. The greater the load on the floor, the greater the stress of the floor member and the greater the creep deflection of the floor.

Creep Model and Discussion

The establishment of a creep model can help to explain and observe the mechanical behavior of the specimen. The mechanical behavior observed in the experiment is obviously related to the composition of the structure itself, and a mathematical model that is in good agreement with the experimental data can be used to analyze the real structure.

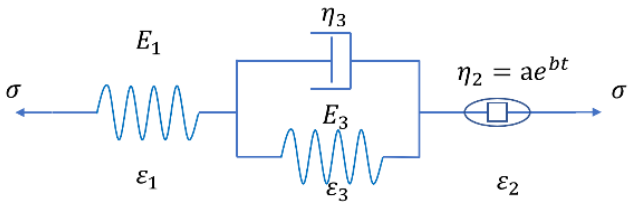

Fig. 12. Modified Burger model with creep for LVL floor

The modified Burger model is composed of a Kelvin model and a Maxwell model in series (Fig. 12) (Liu *et al*. 2021). The creep expression of the model is calculated as follows,

$$\varepsilon(t) = \sigma_0 / E_1 + \sigma_0(1-e^{(-bt)}) / ab + \sigma_0 / E_3(1-e^{(-t/\tau_2)}) \quad (6)$$
$$\tau_2 = \eta_3 / E_3$$

To predict the creep behavior of this model, Eq. 6 was organized into the following forms,

$$f = -Ae^{-Bt} - Ce^{-Dt} + E \quad (7)$$

where t is creep time (Day), while A, B, and C are constants related to materials used as parameters for fitting the equations, where:

$$A = \sigma_0 / E_1,\ B = 1/\tau_2,\ C = \sigma_0 / ab,\ D = b,\ E = \sigma_0 / E_1 + \sigma_0 / E_3 + \sigma_0 / ab \quad (8)$$

According to Fridley *et al.* (1992), when determining the elastic coefficient and viscosity coefficient in Burger model, the change process of humidity and temperature is considered. For this paper, the Burger model transformation equations of Fridley *et al.* (1992) are used for reference. The humidity correlation coefficient w and the temperature coefficient correlation coefficient θ are introduced into the modified Burger model, as follows,

$$\begin{aligned} E_1(w,\theta) &= E_{1s}\left(1 + D_1 w + D_2 w^2 + D_3\theta + D_4\theta^2\right) \\ E_2(w,\theta) &= E_{2s}\left(1 + D_5 w + D_6 w^2 + D_7\theta + D_8\theta^2\right) \\ \eta_1(w,\theta) &= \eta_{1s}\left(1 + D_9 w + D_{10} w^2 + D_{11}\theta + D_{12}\theta^2\right) \end{aligned} \quad (9)$$

where E_{1S}, E_{2S}, and η_{1s} are the elastic and viscous coefficients in the three parameter model, as well as the elastic and viscous coefficients of the reconstituted floor prior to testing. D_1 through D_{12} are the model constants, w are the relative humidity correlation coefficients, θ are the temperature correlation coefficients, and E_1, E_2, and η_1 are the elastic coefficients and viscosity coefficients of the historical process taking into account the humidity and temperature.

Wood's mechanical properties are affected by moisture content and temperature. In the previously defined three-element model, E_1, E_2, and η_1 must be adjusted for their hygrothermal states. In order to accomplish this, two non-dimensional factors are introduced,

$$w = \frac{M - M_0}{M_0} \quad (10)$$

$$\theta = \frac{T - T_0}{T_0} \tag{11}$$

where M denotes humidity reading (%), M_0 represents reference humidity reading (%), T is temperature reading (°C), and T_0 denoted reference temperature reading (°C).

Bringing the initial strain value into Eq. 7, Microsoft Excel 2016 (Microsoft Corp., Redmond, WA, USA) was used to obtain the creep fitting equation of floor (Table 3, Fig. 13).

Table 3. Initial Deflection of Fitting Equation of Creep of Floor

Specimen	Fitting Equation	Fitting Degree (R^2)
L1-1	$f = -1.1436e^{-0.0568t} - 2.7705e^{-0.0014t} + 14.2698$	0.9730
L2-1	$f = -0.5001e^{-0.0707t} - 3.9754e^{-0.0039t} + 14.3893$	0.9592
L2-2	1st loading Same as L1-1 2nd loading $f = -0.6535e^{-0.0152t} - 1.6488e^{-0.0010t} + 15.8559$	0.9730 0.9380
L2-3	$f = -0.7536e^{-0.0817t} - 4.2589e^{-0.0098t} + 22.6605$	0.9631

Figure 13 shows that the fitting equation at the creep stability stage were in good agreement with the creep test value, indicating that the fitting equation can fully reflect the creep performance of Poplar LVL orthogonal ribbed box floor. It should be noted that the fitting equation of specimen L2-1 with local damage was not representative, and this specimen was only used to verify the effect of initial damage on creep performance. The creep equation of specimen L2-2 reflects the influence of repeated load, and its creep equation at the first loading was the same as that of specimen L1-1.

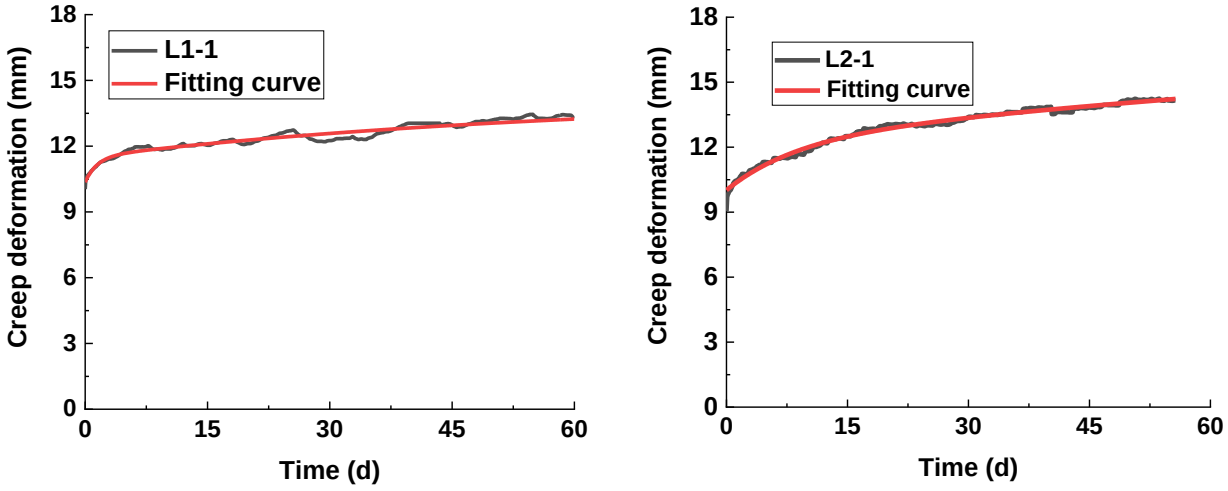

(a) Specimen L1-1 (b) Specimen L2-1

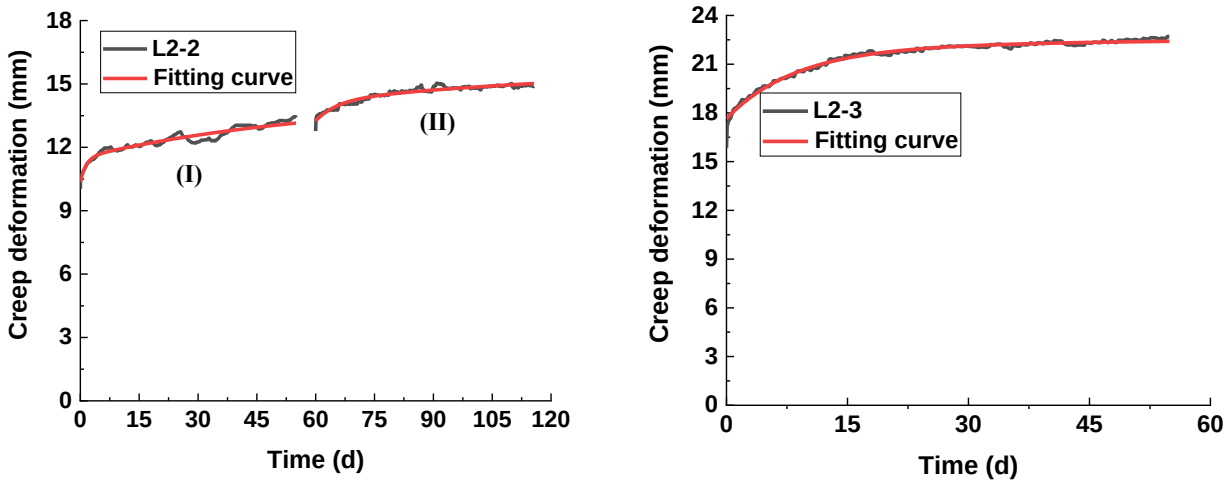

(c) Specimen L2-2 (d) Specimen L2-3

Fig. 13. Comparison of the three-parameter fitting equation with experimental values: (a) Specimen L1-1; (b) Specimen L2-1; (c) Specimen L2-2; (d) Specimen L2-3;

To simplify and facilitate engineering application, the creep fitting equation of Poplar LVL orthogonal ribbed box floor with stress ratio less than or equal to 0.5 is given as follows,

$$\begin{aligned} f &= Ae^{-0.0692t} + Be^{-0.0056t} + C \\ A &= 1.9500n - 1.7286 \\ B &= -7.4420n - 0.5379 \\ C &= f_0 - A - B \end{aligned} \tag{12}$$

where f_0 is initial creep deformation, A , B and C are equation coefficients (see formula 8 for details), t is time (day), and n is the stress ratio. This formula was derived from the test results based on an environment of 6.2 °C to 14.2 °C (temperature) and 33% to 98% (humidity).

When the load is 2.5kN/m^2 (the value of floor live load in Chinese code), the stress ratio at this time is 0.16. According to Eq. 12, the deflection of the creep stability period of the orthogonal ribbed box floor can be calculated as follows:

$$f = -1.4036e^{-0.0692t} - 1.7782e^{-0.0056t} + 7.6830 \tag{13}$$

When t=50 (year), the creep deformation value of the box floor calculated according to formula 13 is 7.68 mm, which is far less than the allowable value of the Chinese code under the standard live load of 2.5 kN/m^2: 14.40 mm.

CONCLUSIONS

1. Loading following local damage, repeated loads, and different stress ratios were used to study the long-term creep properties of poplar laminated veneer lumber (LVL) orthogonal rib box floors. These characteristics are consistent with the general creep law of wood. The creep rate gradually decreases during the first stage of creep; the floor enters the second stage of creep, namely creep stability. With the passage of time, the creep deformation value tends to be stable.
2. Under the same load conditions, the stiffness of the floor slab of the specimen with local damage decreases, the creep deformation increases. Therefore, it is necessary to prevent the floor slab from being damaged in order to improve its mechanical performance.
3. Under repeated load, the viscoelastic deformation after the first unloading accumulates into the viscoelastic deformation after the second loading, which makes the creep deformation of the sample increase slightly, and repeated load has a certain influence on the creep deformation.
4. When the stress ratio increases, the creep rate and creep deformation of the specimen increase, and the magnitude of the load has the greatest influence on the creep deformation of the specimen. When the stress ratio in this study is 0.5, the load reaches 7.5 kN/ m^2, and the creep of the specimen tends to stabilize after a certain time. It can be determined that the box floor has good working performance and stiffness under the load specified in the code (far less than 7.5 kN / m^2).
5. Based on the rheological properties of wood materials, a creep theoretical model is developed for poplar LVL orthogonal rib box floors. The improved Burger model is in good agreement with the experimental results, and it can be used to calculate the creep deformation of poplar LVL orthogonal ribbed box floor.

ACKNOWLEDGMENTS

The authors thank the National Science Foundation of China. This research was funded by the National Science Foundation of China in 2019 (Grant No. 51878590).

REFERENCES CITED

Aipo, M. (2000). "Creep of timber during eight years in natural environments," *Proceedings of the World Conference on Timber Engineering.*

Armstrong, L. D., and Christensen, G. N. (1961). "Influence of moisture changes on deformation of wood under stress," *Nature* 191(7), 869-870. DOI: 10.1038/191869a0

Armstrong, L. D., and Kingston, R. S. T. (1960). "Effect of moisture changes on creep in wood," *Nature* 185(4716), 862-863. DOI: 10.1038/185862c0

Cao, L. (2017). *Research on Mechanical Properties of Larch Plywood Beam*, Master's Thesis, Central South University of Forestry and Technology, Changsha, China. (in Chinese)

Chen, H. (2017). *The Long-term Bending Performance of Controllable Reinforced Plywood Beams Based on Creep Effect*, Master's Thesis, Northeast Forestry University, Harbin, China. (In Chinese)

Dinwoodie, J. M., Higgins, J. A., and Paxton, B. H. (1992). "Creep in chipboard," *Wood Science & Technology* 26(5), 429-448. DOI: 10.1007/BF0022947

Fridley, K. J., Tang, R. C., and Soltis, L. A. (1992). "Creep behavior model for structural lumber," *Journal of Structural Engineering* 118(8), 2261-2277. DOI: 10.1061/(ASCE)0733-9445(1992)118:8(2261)

He, T. (2016). *Study on Long-term Bending Performance of Prestressed Glued Bamboo-wood Beam based on Creep Effect*, Master's Thesis, Northeast Forestry University, Harbin, China. (In Chinese)

Jozsef, B., and Benjamin, A. J. (1982). *Mechanics of Wood and Wood Composites*, Van Nostrand Reynold Company Inc.

Leichti, R. J., and Tang, R. C. (1989). "Comparative performance of long-term loaded wood composite I-beams and sawn lumber," *Wood and Fiber Science* 22(21), 142-154. DOI: 10.1515/hfsg.1989.43.2.141

Liu, F. W. (2018). *Study on the Mechanical Properties of Poplar Plywood Beam under Long-term Load*, Master's Thesis, Yangzhou University, Yangzhou, China. (In Chinese)

Liu, Y., Wang, H. H., and Ding, P. R. (2017). "Physical and mechanical properties of poplar veneer plywood," *Forest Industry* 44(02), 12-16. DOI: 10.19531/j.issn1001-5299201702003 (in Chinese)

Liu, Y., Jia, W. B., Su, X. Y., Ma, H. W., and Xiao, Z. P. (2021). "Assessing the creep performance of full-scale bamboo scrimber column," *BioResources* 16(2), 3691-3705.

Pierce, C. B., Dinwoodie, J. M., and Paxton, B. H. (1979). "Creep in chipboard. The use of fitted response curves for comparative and predictive purposes," *Wood Science and Technology* 13(4), 265-282. DOI: 10.1007/BF00356969

Schniewind, A. P. (1967). "Creep-rupture life of Douglas-fir under cyclic environmental conditions," *Wood Science and Technology* 1(4), 278-288. DOI: 10.1007/BF00349759

Sheng, X. Q. (2015). *Study on the Creep Property of Laminated Veneer Lumber*, Master's Thesis, Yangzhou University, Yangzhou, China. (in Chinese)

Su, X. Y., Chen, J., Liu, Y., Sun, X. Y., Gong, M., and Wang, H. D. (2022) "Experimental study on flexural behavior of box floors with orthogonal rib beams made of poplar laminated veneer lumber," *BioResources* 17(4), 6019-6035. DOI:10.15376/biores.17.4.6019-6035

Wang, Z. L., Liu, W. Q., and Xu, Q. F. (2020). "Experimental study on the mechanical behavior of wood beams strengthened with CFRP bars under load for 6 years," *Building Structure* (05), 15-19+14. DOI: 10.19701/j.jzjg. 2020.05.003. (in Chinese)

Yang, Y. (2017). *Short-term Loading Test of Prestressed Plywood Beam String Based on Sowing Effect*, Master's Thesis, Northeast Forestry University, Harbin, China. (in Chinese)

Yazdani, N., Johnson, E., and Duwadi, S. (2003). "Creep effect in structural composite lumber for bridge applications," *Journal of Bridge Engineering* 9(1), 87-94. DOI: 10.1061/(ASCE)1084-0702(2004)9:1(87)

Zhou, J. R., Li, Y. S., and Wang, J. L. (2020). "Mechanical properties of steel-bamboo composite slabs under long-term load," *Forest Engineering* 36(01), 109-114. DOI: 10.3969/j.issn.1006-8023.2020.01.015 (In Chinese)

Zhu, E. C., and Zhou, H. Z. (2009). "Creep buckling of plywood timber arch," *Journal of Shenyang Jianzhu University* 25(4), 640-643. DOI: CNKI:SUN:SYJZ.0.2009-04-006. (In Chinese)

Zuo, H. L., Hu, B., and Liu, H. R. (2021). "Effect of creep on long-term bending performance of reconstituted bamboo board reinforced plywood beams," *Journal of Northeast Forestry University* 49(12), 115-119. DOI: 10.13759/j.cnki.dlxb.2021.12.005 (In Chinese)

Article submitted: July 6, 2022; Peer review completed: September 3, 2022; Revised version received and accepted: September 13, 2022; Published: September 16, 2022.
DOI: 10.15376/biores.17.4.6158-6177